



# HASP Student Payload Application for 2021

Payload Title: Flight test of the University of the Virgin Islands Gamma-Ray Experiment for Astrophysical Transients (UVI-GREAT)	
Institution: University of the Virgin Islands	
Payload Class (Enter SMALL, or LARGE): <b>Small</b>	Submit Date: 01-07-22
<p>Project Abstract:</p> <p>Gamma-ray bursts (GRBs) are among the most energetic events in the Universe and are associated with gravitational waves, opening a new observational window into the Universe. Detection of GRBs is currently done by NASA's Neil Gehrel's Swift Observatory and Gamma-ray Space Telescope. These missions will eventually end, leaving a need for GRB detection capability in space. Gamma-ray detecting cubesats represent a potential low-cost, low-risk alternative to larger, more costly missions. Several groups around the world are working on GRB-detecting cubesats. We will build and fly a prototype GRB-detecting instrument in an approximate 3U cubesat frame as a pathway to developing a future gamma-ray detecting cubesat. This HASP instrument is a technology demonstration mission (demonstrating the use of silicon photomultipliers for GRB detection) and a capability demonstration mission (demonstrating the ability of the University of the Virgin Islands, a small HBCU, to build a successful astrophysics mission). The instrument will be designed to demonstrate GRB detection in the 10-1000 keV energy range. Due to the short time of the HASP flight, however, a GRB is unlikely to be detected, so we will optimize this instrument for observations of the Crab Nebula, the brightest steady gamma-ray source in the northern sky.</p>	
Team Name: University of the Virgin Islands Gamma-Ray Experiment for Astrophysical Transients (UVI-GREAT)	Team or Project Website:
Student Leader Contact Information:	Faculty Advisor Contact Information:
Name: Peter Jean-Baptiste	David Morris
Department: Chemical and Physical Science	Chemical and Physical Science
Mailing Address: 2 John Brewer's Bay	2 John Brewer's Bay
City, State, Zip code: St. Thomas, USVI 00802	St. Thomas, USVI 00802
e-mail: pjay2540@gmail.com	dmorris@uvi.edu

Office Telephone:	3406265800	6176101148
Mobile Telephone:	3406265800	6176101148

## Flight Hazard Certification Checklist

NASA has identified several classes of material as hazardous to personnel and/or flight systems. This checklist identifies these documented risks. Applying flight groups are required to acknowledge if the payload will include any of the hazards included on the list below. Simply place an (x) in the appropriate field for each hazard classification. **Note:** Certain classifications are explicitly banned from HASP (grey filled items on table below) and the remaining hazards will require additional paperwork and certifications. If you intend to include one of the hazards, you must include detailed documentation in section 3.8 of the application as required by the HASP Call for Payloads.

This certification must be signed by both the team faculty advisor and the student team lead and included in your application immediately following the cover sheet form.

<b>Hazardous Materials List</b>		
<b>Classification</b>	<b>Included on Payload</b>	<b>Not Included on Payload</b>
RF transmitters		<b>X</b>
High Voltage		<b>X</b>
Pyrotechnics		<b>X</b>
Lasers		<b>X</b>
Intentionally Dropped Components		<b>X</b>
Liquid Chemicals		<b>X</b>
Cryogenic Materials		<b>X</b>
Radioactive Material		<b>X</b>
Pressure Vessels		<b>X</b>
Magnets		<b>X</b>
UV Light		<b>X</b>
Biological Samples		<b>X</b>
Li-ion Batteries	<b>X</b>	
High intensity light source		<b>X</b>

Student Team Leader Signature:

-

*Peter Jean-Baptiste*

Faculty Advisor Signature:

-

*David C. Morris*

# Table of Contents

Flight Hazard Certification Checklist.....	2
Table of Contents.....	4
1. Payload Description.....	5
1.1 Payload Scientific / Technical Background.....	5
1.1.1 Mission Statement.....	7
1.1.2 Mission Background and Justification.....	7
1.1.3 Mission Objectives.....	8
1.2 Payload Systems and Principle of Operation.....	9
1.2.1 Gamma-Ray Detector Payload.....	9
1.2.2 Mechanical Structure.....	13
1.2.3 Computer systems and software.....	13
1.2.4 Electrical and Power Systems.....	16
1.3 Thermal Control Plan.....	18
1.3.1 - Simple analytical equilibrium thermal calculation.....	19
1.3.2 - Thermal Testing Plan.....	20
2. Team Structure and Management.....	20
2.1 Team Organization and Roles.....	20
2.2 Timeline and Milestones.....	22
2.3 Anticipated Participation in Integration and Launch operations.....	23
3. Payload Interface Specifications.....	23
3.1 Weight Budget and Power Budget.....	23
3.2 Downlink Serial Data.....	23
3.3 Uplink Serial Commanding.....	24
3.4 Analog Downlink.....	24
3.5 Discrete Commanding.....	24
3.6 Payload Location and Orientation Request.....	24
3.7 Special Requests.....	25
4. Preliminary Drawings and Diagrams.....	26
5. References.....	28
Appendix.....	29

# 1. Payload Description

Gamma-ray bursts (GRBs) are some of the most energetic events in the Universe and are associated with the production gravitational waves, opening an entirely new observational window into the Universe. Detection of gamma-ray bursts is currently done by NASA's Neil Gehrel's Swift Observatory and NASA's Fermi Gamma-ray Space Telescope. These missions will eventually end, however, and the need for follow-on gamma-ray detecting capability in orbit will become great. Gamma-ray detecting cubesats represent a potential low-cost, low-risk alternative method of gamma-ray burst detection to larger, more costly missions. Several groups around the world are working on gamma-ray burst detecting cubesat prototype missions. Here, we propose to build and fly a prototype gamma-ray burst detecting instrument in an approximate 3U cubesat frame as a pathway instrument to developing a future gamma-ray detecting cubesat. This HASP instrument is both a technology demonstration mission (demonstrating the capability of using silicon photomultiplier technology for GRB detection) and a capability demonstration mission (demonstrating the ability of the University of the Virgin Islands, a small liberal arts HBCU, to build a successful astrophysics mission). The instrument will be designed to demonstrate gamma-ray burst detection capability in the 10-1000 keV energy range. Due to the short duration of the HASP flight, a GRB has a relatively low likelihood of being detected, thus we will optimize this demonstrator instrument to make observations of the Crab Nebula, the brightest steady gamma-ray source in the northern sky.

## 1.1 Payload Scientific / Technical Background

The UVI-GREAT mission is a technology demonstration and infrastructure and student development program at the University of the Virgin Islands that will help to demonstrate the value of flying multiple, low-cost, gamma-ray detecting instruments (eventually in cubesat payloads) as a low-cost, low-risk alternative to larger gamma-ray burst detecting missions like the NASA Neil Gehrel's Swift Observatory and Fermi Gamma-ray Space Telescope. Low-cost gamma-ray detecting cubesats are unlikely to be equipped with coded-aperture masks or have other techniques for producing gamma-ray images. Therefore, in order for a group of small gamma-ray detecting cubesats to effectively locate gamma-ray bursts with sufficient spatial resolution to enable ground-based optical followup (as is currently done with arc-second precision locations from Swift), several cubesats will need to detect the GRB simultaneously so that photon time-of-flight can be used to effectively triangulate a high precision sky location. To achieve this, several groups around the world are working on building such cubesats and more will be needed to improve positional accuracy. UVI has partnered with collaborators at Goddard Space Flight Center to build a prototype GRB-detecting instrument leveraging flight-spare components from previous gamma-ray

balloon and cubesat missions to achieve 2 goals: 1 - to demonstrate an extremely-low-cost, technically capable gamma-ray detecting mission that can achieve GRB detection with commercial off-the-shelf components and that can be designed, bench-tested, assembled, and flight-tested by a team of students with little prior training in cubesat hardware. Developing and demonstrating the capability of such a low-cost, low-technical-entry-point mission will open the possibility for dozens to hundreds of similar missions to be developed and flown from universities across the world; 2 - to train current UVI students and graduates and to establish UVI's aerospace instrumentation laboratory. The UVI instrumentation lab has a several-years collaboration with partners at Goddard Space Flight Center in developing detector testing capability at UVI. This project is the next evolutionary step in UVI's instrument lab development as we now plan to build and test a flight-ready gamma-ray instrument fully in our UVI labs.

To effectively discriminate between gamma-ray bursts and other steady and variable gamma-ray sources in the sky, the UVI-GREAT instrument will need sufficient timing and spectral resolution to distinguish between classes of sources. Moreover, since one of the important goals of modern GRB detection is to search for gravitational wave counterparts, it will be important to be able to distinguish between the long class of GRBs (which come from collapsing massive stars and are not expected to produce detectable levels of gravitational waves) and short GRBs (which come from coalescing compact objects and are expected to produce detectable levels of gravitational waves). The typical separation between short and long GRBs is at 2 seconds (short GRBs  $< 2s$  and long GRBs  $> 2s$ ). Short GRBs also have different spectra from long GRBs, with short GRBs having a higher ratio of higher energy x-ray emission compared to low energy x-rays. This spectral difference is usually classified by the 'hardness ratio'. Short GRBs have a 50-100keV/25-50keV ratio of about 2 while long GRBs have a ratio of about 1. The need to be able to distinguish steady gamma-ray sources from transient gamma-ray sources and to be able to distinguish short GRBs from long GRBs drives our technical parameters. Our goal is to detect gamma-ray sources of approximately 1 Crab intensity ( $10^{-12}$  ergs/cm<sup>2</sup>/s) with 6 sigma detection significance on timescales no longer than 2 seconds and to be able to resolve the photon energies with resolution of at least 25 keV from 10-100keV. This detection level will allow us to distinguish between steady sources like the Crab Nebula and transient sources like blazar flares and GRBs and will further allow us to distinguish between short and long classes of GRBs. Spectral discrimination will also help us to distinguish between classes of sources.

While our ultimate GRB detection cubesat will require higher timing accuracy than the 2 seconds noted here in order to allow high-precision time-of-flight position reconstruction, the short duration of this technology demonstration mission (12-18 hours) makes it rather unlikely that we will detect a GRB. Thus we focus this instrument development activity to achieve the capabilities required to detect a steady gamma-ray source, the Crab Nebula, with sufficient timing and spectral resolution to distinguish it from other

sources (including the unlikely though not impossible detection of a GRB). The Crab Nebula is chosen as our target due to the fact that it is the brightest source in the sky in the energy range of interest (10~1000keV) and because it is well isolated from other bright hard x-ray sources in the sky, making it a convenient target to act as a “pseudo-GRB”, that is, a hard x-ray source that is much brighter (more than x10 in the band of interest) than other sources in the sky. Based on an expected HASP flight in mid-August 2022 from Fort Sumner, NM, we expect the Crab Nebula to be directly overhead at approximately 9am. Assuming an early-morning launch of the HASP gondola, we expect to collect sufficient on-flight data to distinguish the Crab Nebula flux level and spectral hardness ratio in the 50-100/25-50 keV band and to distinguish when the Crab Nebula passes out of view when it sets below the horizon.

### 1.1.1 Mission Statement

The University of the Virgin Islands Gamma-Ray Experiment for Astrophysical Transients (UVI-GREAT) is designed to test and validate the performance of a compact, low-cost gamma-ray burst detection instrument. Similar instruments are being developed by several groups as potential low-cost replacements to current gamma-ray transient detection missions like the Neil Gehrels Swift Observatory.

### 1.1.2 Mission Background and Justification

GRBs come from 2 general classes of sources, ‘long’ GRBs from the collapse of supermassive stars, and ‘short’ GRBs from the coalescence of compact objects. While we are interested to detect and understand both classes, the latter class is associated with gravitational wave sources and thus we are especially motivated to ensure that our instrument can detect the difference between short and long GRBs. The timing and ‘hardness ratio’ differences between long and short GRBs is shown in the figure below:

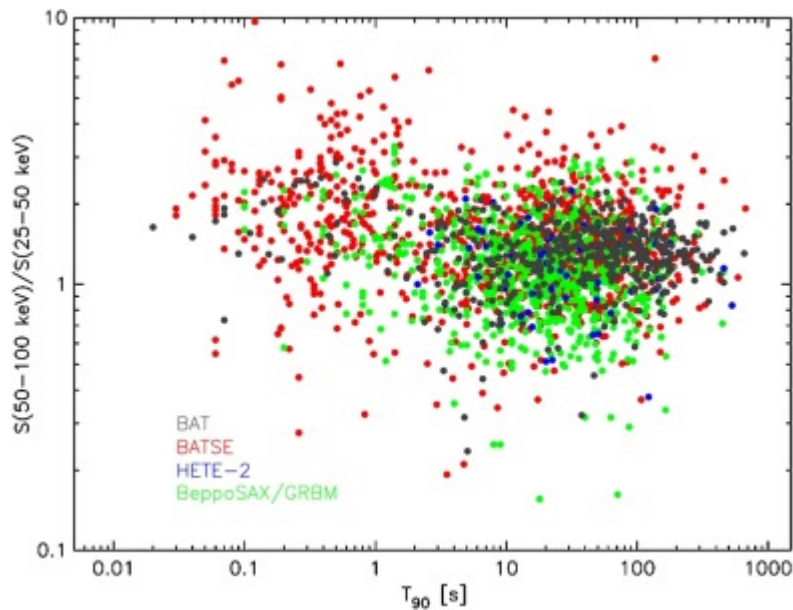


Figure 1 – Timing and hardness of GRBs [1]

Because GRBs are divided into 2 groups with separation in timing (with a break between groups at about 2s) and with separation in spectrum (with a difference in hardness ratio of roughly 2 compared to 1.5), our instrument is designed to detect GRBs with a 6 sigma detection confidence on 2s integrations and with spectral energy resolution of 25 keV over the energy band from 10-1000 keV. These capabilities allow us to distinguish GRBs from other constant gamma-ray sources in the sky and also allow us to distinguish short GRBs from long GRBs.

### 1.1.3 Mission Objectives

Minimum Success criteria:

Our minimum success criteria for the UVI-GREAT mission are:

- the instrument is successfully be delivered and approved for flight
- the instrument successfully powers on

Moderate Success criteria:

- Above criteria and:
- System records data to the flash drive
- Data are successfully recovered for analysis

High Success criteria:

- Above criteria and:
- System records at least one gamma-ray event on orbit

Complete Success criteria:

- Above criteria and:
- System operates for entire flight
- Gamma-ray excess detected during time period when Crab nebula is visible

## 1.2 Payload Systems and Principle of Operation

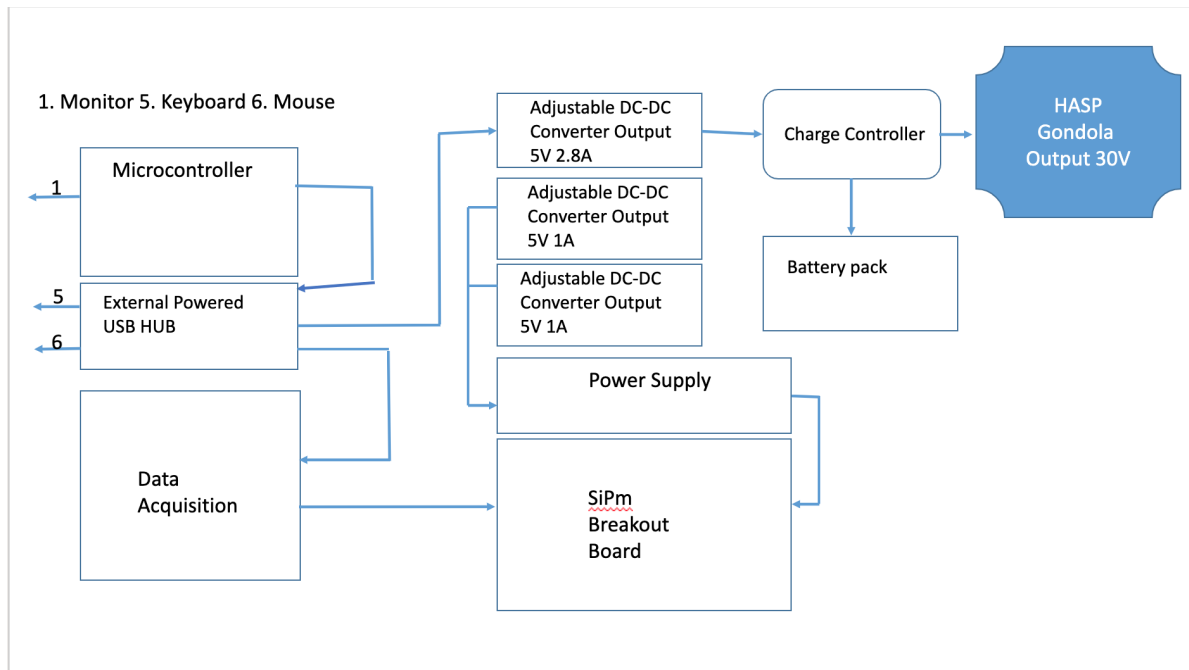


Figure 2 – System block diagram of payload

A high-level diagram of the system is shown in figure 2 (above). The instrument consists of a CsI(Tl) scintillator crystal bonded to a 4x4 silicon photomultiplier (SiPM) array. The 16 SiPMs are mounted to 2x2 carrier boards which are then mounted in a 2x2 pattern (resulting in an overall 4x4 arrangement) on the front-end electronics (FEE) assembly. The FEE mounts to a standard pc104 board which is mounted to aluminum rails attached to the walls of the instrument frame. The FEE is read out through a high-speed (1 Gbps) analog to digital converter (ADC) which connects to a microcontroller to store the data. This microcontroller also acts as the onboard flight computer including temperature monitoring and communications. Power is supplied by means of an on-board 30Whr battery-pack that is connected to the HASP power mains supply through a LTC4020 charge controller board that is mounted to a DC-DC converter board. The DC-DC converter board is protected from the downstream computer and detector components by an overcurrent protection circuit.

### 1.2.1 Gamma-Ray Detector Payload

The gamma ray instrument onboard the UVI-GREAT project will be used to detect gamma ray bursts in the 10-1000 keV band at 2s intervals and will monitor the gamma ray sky for transient and steady gamma-ray sources. The detector assembly will consist of a thallium-doped cesium iodide (CsI(Tl))

scintillating crystal coupled to a 4x4 silicon photomultiplier (SiPM) on front-end electronic (FEE) board. The FEE used here will be a flight spare boards from the Ionospheric Neutron Content Analyzer (INCA) experiment used by the New Mexico State University team in collaboration with Goddard Space Flight Center. The principle of operation of the detector is:

ultraviolet light generated by gamma ray photons colliding in the scintillating crystal are converted into electrical pulses through the 4x4 SiPM array connected to the FEE board. Data will be read out through the FEE board to an analogue to digital converter (ADC) board that is controlled through a microcontroller running the instrument control software. The ADC board will read out the analog signal from one channel and convert the signal to digital. The microcontroller is an open-software computer with 1GHz processing speed, 512MB DDR3 RAM, 4GB on-board storage and a microSD card slot. This computer is capable of running the flight software required to save and analyze the data collected by the DRS4 evaluation board and will provide timestamps for each data packet.

While our instrument is ultimately designed to detect and characterize gamma-ray bursts, the probability to detect a GRB during this prototype balloon flight is low given the relatively short flight duration. GRBs with sufficient brightness to be detected by our detector are expected to occur approximately once per week. Thus for a flight duration of approximately 15 hours, we expect a probability (assuming a Poisson distribution of events) of 8% to detect a GRB. Thus, to ensure detection of an astrophysical gamma-ray source to demonstrate the performance of our instrument, we will optimize this version of our instrument to detect the brightest constant gamma-ray source in the sky, the Crab Nebula, with sufficient signal to noise ratio to distinguish between periods of the flight when the Crab nebula is in view and periods when it is not. To determine the size of the scintillating crystal needed for measurements, the brightness of the Crab nebula needs to be compared to the background at the float altitude at which the HASP will operate. Based on two figures below, we will integrate the signal and background count rates between the energy range of 20-100 keV. The next step is to work backwards to calculate the size of the crystal needed to achieve a detection of the Crab signal at our desired confidence level. We will use 4-sigma above background (99.99% confidence) as our detection level criterion. Assuming that our background noise level is Gaussian, we have that:

$$\frac{Signal}{\sqrt{Background}} = 4$$

where

$$Signal = (Crabrate) \times (crystal\ effective\ area) \times (time)$$

and

$$Background = (background\ rate) \times (crystal\ effective\ area) \times (time)$$

Figure 3 (below) shows the expected 10-250keV spectrum of the Crab Nebula while Figure 4 shows the expected hard X-ray background in the same spectral range. We numerically integrate these source and background curves to find that the Crab emission from 20-100keV is 0.938 cts/cm<sup>2</sup>/s and the background rate is 0.325 cts/cm<sup>2</sup>/s in the same spectral range.

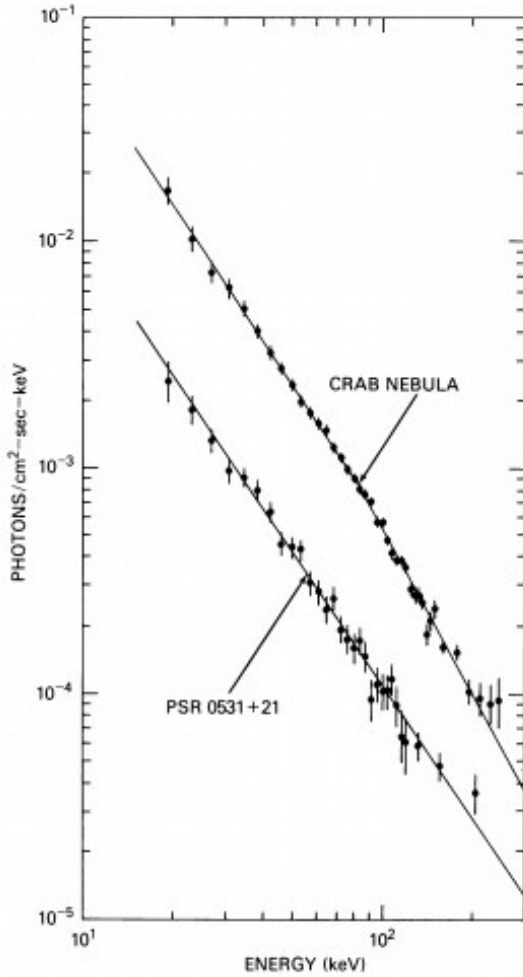


Figure 3: Hard X-ray Spectrum of the Crab Nebula (top curve) [2].

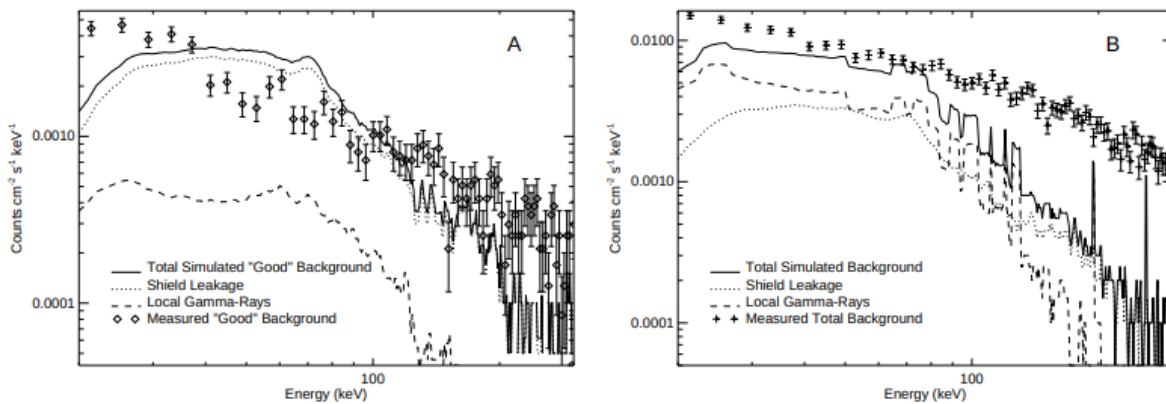


Figure 4: Background Gamma-Rays measured at an altitude of 25 miles [3].

Solving the above equation, we find:

$$A(t) = \frac{16 \times 0.325 \frac{\text{cts}}{\text{cm}^2 \text{s}}}{\left(0.938 \frac{\text{cts}}{\text{cm}^2 \text{s}}\right)^2} = \frac{5.54}{t} \text{cm}^2 \text{s}$$

for a 4-sigma detection over a time interval of 't' seconds. Thus, for integration times of 2 s, we calculate a required effective area of 2.77 cm<sup>2</sup>.

Based on GEANT simulations performed by the Burstcube instrument team for a similar detector layout using CsI [4], we can extrapolate an effective area for our instrument from the crystal size of their cylindrical CsI(Na) scintillators. Using similar crystal configurations and SiPMs, Burstcube has an effective area of 65 cm<sup>2</sup> at 100 keV using a crystal footprint of about 254 cm<sup>2</sup>. UVI-GREAT's crystal size will then need to be

$$\frac{2.77 \text{ cm}^2}{65 \text{ cm}^2} \times 254 \text{ cm}^2 = 10.8 \text{ cm}^2$$

Our planned crystal size will cover the 4 cm x 4 cm SiPM array and therefore have a crystal size of approximately 16 cm<sup>2</sup>, exceeding the required size calculated here.

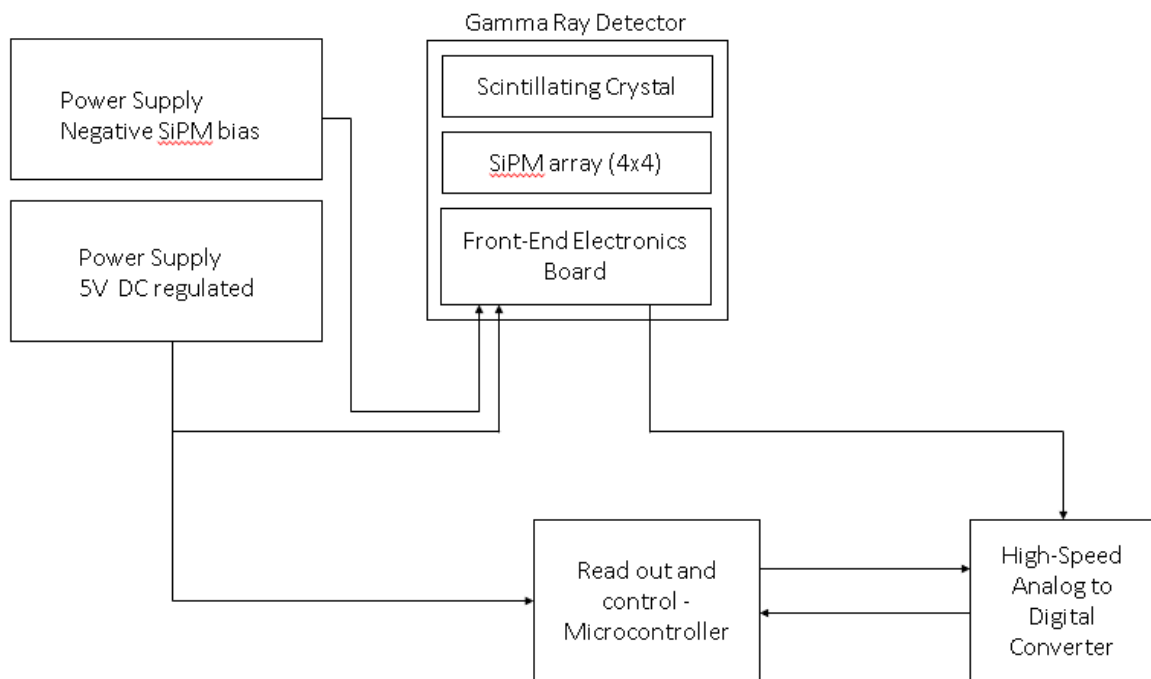


Figure 5: Block diagram of gamma-ray detection system.

## 1.2.2 Mechanical Structure

The UVI-GREAT Structure is composed of 6061-T6 aluminum that is in a 3U-Cubesat formation. It begins with a structured skeleton, which houses a primary and secondary base level, as well as a top cover. There are four wall panels, which are attached to the structure to increase its mechanical strength and allow ease of access to the internal payload. The structure is held together by thirty blind rivets. Six rivets on each wall, excluding the front panel, are binding with each respective 3-U rail. There are four blind rivets on each base level, as well as the top cover. There are also fourteen # 8-32 UNC carbon steel flat head Rivnuts, which are threaded with a knurled body. Ten are used on the front panel, attached to their respective rails. The remaining four are attached to the 3U frame base, which will be used to connect the base to the HASP Plate. Pan Head, Phillips-slotted, one inch # 8-32 screws are placed into the ten rivnuts. The structure will be wrapped in Kapton tape, to assist in constant thermal control over the internal payload.

## 1.2.3 Computer systems and software

The onboard computer system will be a low-cost, off-the-shelf microprocessor (for example, a Raspberri Pi or Beaglebone processor). This microprocessor will be connected to a USB hub to allow connection of peripheral devices like keyboards and mice for testing purposes and check-out prior to launch. The USB hub will also connect to a flash memory drive that will serve as the hard drive to store data collected by our gamma-ray instrument.

The onboard software control loop is shown in figure 6 below. When the instrument is powered up, the instrument control software is automatically started by linux boot script. The linux script file executes the following instructions: the first one is to detect if the microprocessor was powered with the required voltage and amperage. Second: after successful boot of the linux Debian operating system, the watchdog timer is activated, this timer is used to detect and recover from any microprocessor run errors. Watchdog timers are widely used in embedded systems to facilitate automatic correction of temporary hardware faults, and to prevent errant or malevolent software from disrupting system operation. During normal operation, the microprocessor regularly restarts the watchdog timer to prevent it from elapsing, or "timing out". If, due to a hardware fault or program error, the microprocessor fails to restart the watchdog, the timer will elapse and generate a timeout signal. The timeout signal is used to initiate corrective actions. The corrective action is to force the microprocessor to reboot. In step three, the executable file program represented by the flowchart of figure 6 is run, this program samples the ADC readout which carries the signal coming from the output of the gamma-ray detector board. Fourth: the watchdog timer is restarted and step three is repeated (and looped). If the watchdog timer is not successfully reset, then the system is forced to reboot. The program does not have an ending because it will run in an infinite loop until the end of the flight or until a command is sent to reboot the system.

Figure 6 shows the program to sample the signal from the ADC. The first steps are the software driver initialization, then the configuration of the input range voltage, sampling frequency, and trigger level. After the signal reaches the trigger level, then the incoming pulse is stored into an array with size of 1024 samples, and the data points are saved into the flash hard drive card as a plain ascii text file.

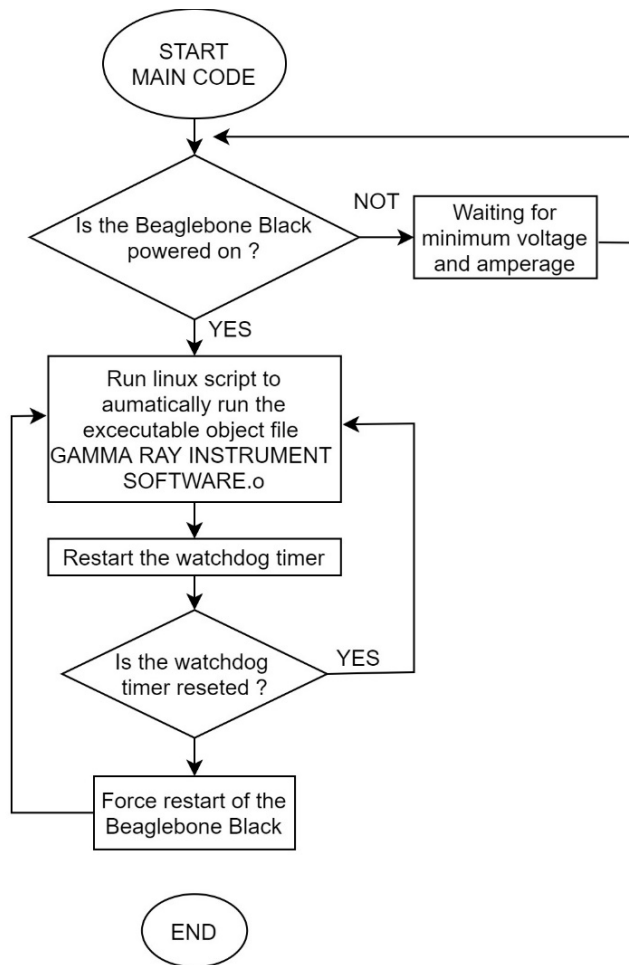


Figure 6 – Flight software block diagram

Analysis of our data to reconstruct the energy and timing of individual photons will occur after the flight, using the ‘ground analysis software’. This will be a python script that takes an array of peak voltages of gamma ray events and creates a histogram plot of peak heights. To do so, the python script reads the data file stored on the flash drive containing the ADC output data from the detector. This file contains time and amplitude data for multiple waveforms captured by the ADC. The python script then saves the peak value in the waveform of each gamma ray event and saves the values to a list. The list is then used to create histogram plots using standard python

matplotlib libraries. The program also fits a Gaussian curve to any identified spectral features. This function will be useful during the calibration phase of the commissioning to determine the gain of the detector, though we do not expect to detect any spectral line features in sources detected on orbit. The code then returns the histogram plot along with the parameters of the Gaussian fit (amplitude, centroid, and line width) and the uncertainties of the fit parameters. The Gaussian fits to photopeak spectral features of known calibration sources are used to determine the instrumental energy gain and energy resolution calibration.



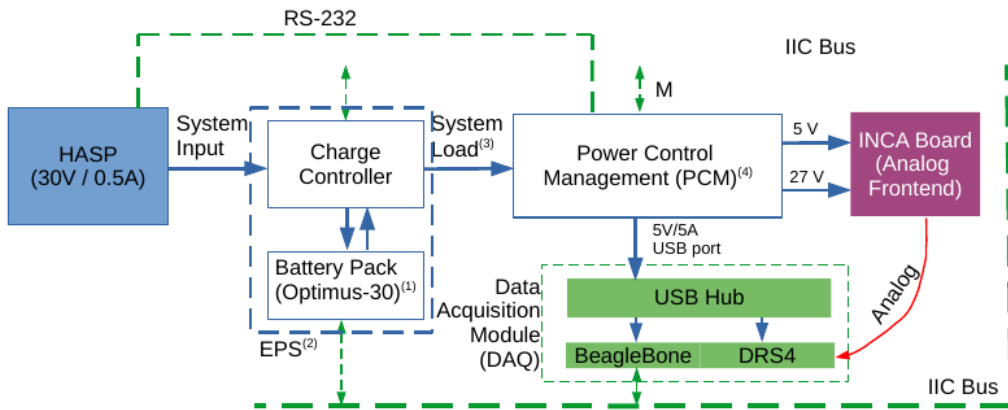
Figure 7 – Analyze spectra function

## 1.2.4 Electrical and Power Systems

The electrical and power system top-level design is shown below in figures 8 and 9. The power supply for the UVI-GREAT project is based on the AAC Clyde nano-pico EPS and AAC Clyde battery packs. The reason for using the AAC Clyde EPS system is that it could be reused in future efforts to build a CubeSat since it is space qualified (see certificate of conformance for ISS manned space flight included in appendix).

The AAC Clyde EPS and its battery pack is a fairly complete design for an EPS system with charge controller, 3 output power rail at 12V, 5V, and 3.3V, controlled interface, etc. Ideally, it can just work out of the box without any modifications or any additional design. However, we expect that some UVI-GREAT system components will not be cubesat standard compatible components (in terms of voltages, and connectors) and thus may not interface seamlessly to the AAC Clyde system. Moreover, the analog circuit will need a high voltage power supply for biasing the SiPM sensor (up to 27V, not exceeding 50V and thus not listed in the 'hazardous materials' list) and this voltage needs to be clean. Therefore, an additional power supply board needs to be designed to work in tandem with the AAC Clyde EPS board. This board is called Power Control Management (PCM).

The PCM board takes three power rails from EPS to generate power supply for the data acquisition part, analog board operational amplifiers supply, and analog board high voltage. The 12V rail is put through a DC/DC converter to generate 5V for data acquisition parts. The reason for using 12V rail instead of using directly 5V rail is that it will use less current from the rail. The 5V rail from AAC EPS is used to power analog boards. High voltage for biasing the SiPMs will be generated by an off-the-shelf SiPM power supply like the CAEN A7585 module, which is a specialized voltage regulator for SiPM biasing. The 12V and 5V rail from the EPS is monitored and protected by a smart power switch like the Texas Instruments TPS27S100 and a current sense amplifier. The whole system on the PCM board is monitored and controlled by a housekeeping microcontroller. Power for this microcontroller comes directly from the battery so that it can work even in the absence of an external power supply in case of momentary power interrupts from the HASP.



- (1): Battery Pack Optimus-30:
- Charge voltage: 8.4V (max), 8.26V (nominal)
  - Discharge voltage: 6.2V
  - Charge/Discharge current: 1.95A
- (2): Electrical Power System (EPS) is either AAC Clyde full solution or combination of AAC battery and COTS charge controller or full COTS solutions.
- (3): Three voltage comes out of EPS +12V, +5V, +3.3V follow PC104 standard.
- (4): Power Control Management includes:
- DC/DC Converter (5V/5A) for DAQ Module
  - DC/DC Converter (5V/2A) for INCA
  - DC/DC Converter for INCA High voltage biasing (CAEN)
  - Current sensing
  - Over voltage / over current protection
  - Power FET for switching on/off
  - House keeping Microcontroller (master of IIC bus).

Figure 8 – Electrical power system

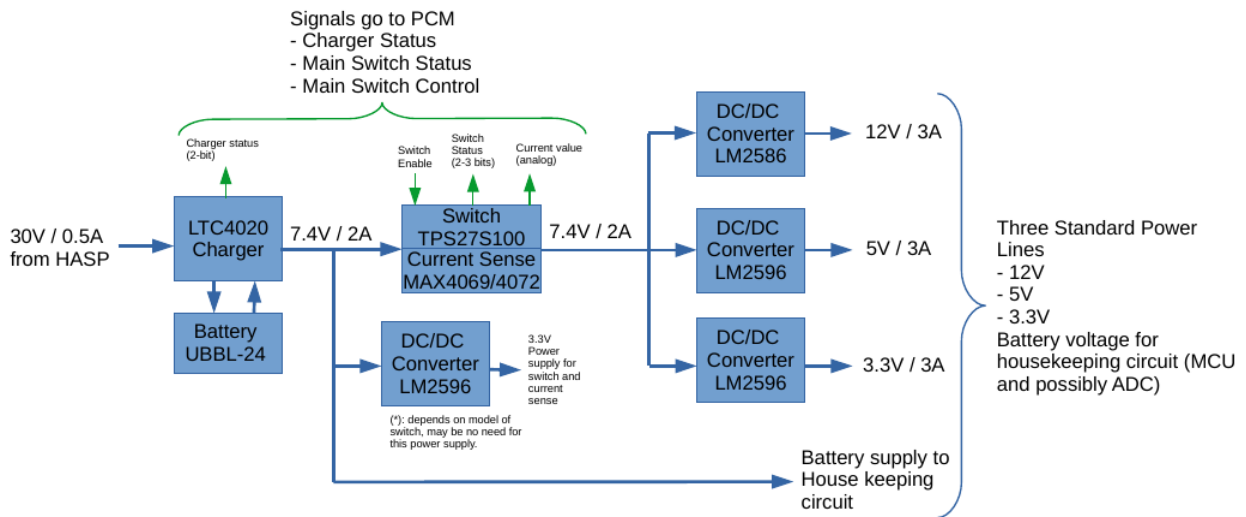
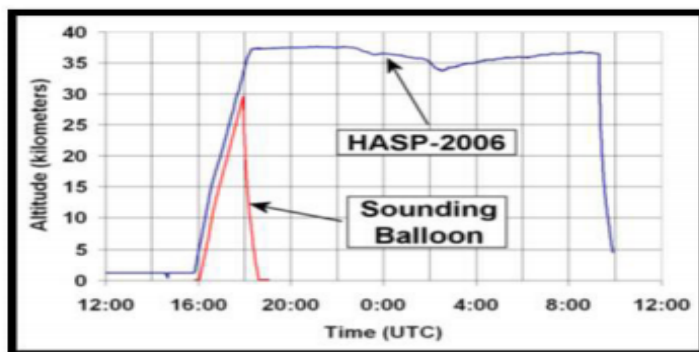


Figure 9 – Electrical power system

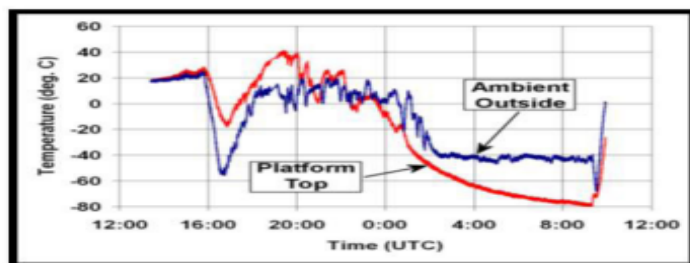
### 1.3 Thermal Control Plan

For a typical HASP balloon flight, the temperature profile is shown figure 9. Our structure must maintain the instrument in an environment that is safe for our electronics to operate and where it can perform to specifications. The expected location for the flight according to HASP documentation is Fort Sumner, New Mexico (Lat, Long 34.47°N, 104.24°W ). The average length of day during August is twelve (12) hours and fifty-four (54) minutes.

The UVI-GREAT HASP payload will be operating within a thermal environment range of  $-60^{\circ}\text{C}$  to  $+40^{\circ}\text{C}$  at an altitude of about 30 to 40 kilometers --as indicated by the pre-observed temperature/altitude profile charts below. The operational temperature range of the component parts (to be discussed further in the payload specifications table, see section 3) are from  $-40^{\circ}\text{C}$  to  $+80^{\circ}\text{C}$ . To help insulate the instrument to maintain the components within their operational temperature ranges, we will layer the instrument frame walls, base and top with Kapton tape inside and outside. Additionally, internal heating mechanisms may be used as secondary protection to keep electronics within survival temperature profiles if it is determined through testing that there is significant concern of temperatures becoming too cold.



A typical altitude vs. time flight profile for HASP compared to that of a sounding balloon flight



Characteristic temperatures outside HASP during the 2006 flight

Figure 9 – Operating environment of HASP [5]

### 1.3.1 - Simple analytical equilibrium thermal calculation

In addition to ensuring that our instrument components are certified to operate in the ambient conditions during the rise and decent phases of the flight, we also have conducted a simple thermal equilibrium analysis at float altitude to determine the expected minimum and maximum operating temperatures at float altitude.

Heat transfer into and out of our instrument will occur through conduction, convection and radiation processes. At float, the low density of the atmosphere will make radiation the dominant heat exchange mechanism. Thus, to obtain a first-order evaluation of expected high and low temperature, we have enlisted a simple thermal equilibrium model assuming radiative heat exchange only. We consider input heat exchange from Solar irradiation ( $Q_{solar}$ ), Earth irradiation (from IR emission,  $Q_{earth}$ ) and Earth reflection of Solar radiation ( $Q_{albedo}$ ). We assume an input power from our instrument of 6.8W as shown in table 3 ( $Q_{generated}$ ). Our calculation is outlined below and summarized in equations presented:

$$Q_{stored} = Q_{in} - Q_{out} + Q_{generated}$$

$$Q_{in} = Q_{solar} + Q_{IR} + Q_{albedo}$$

$$Q_{in} = \alpha \cdot A_{sun} \cdot q_{solar} + \epsilon \cdot A_{earth} \cdot q_{earth} + \alpha \cdot A_{earth} \cdot albedo \cdot q_{sun}$$

$$Q_{out} = \sigma \cdot \epsilon \cdot A \cdot T^4$$

(assumes seeing no other temperature source)

( $\sigma$ : Stephan-Boltzman constant)

$$Q_{stored} = 0$$

Figure 11 – Thermal calculation

Assuming  $Q_{stored} = 0$  we can solve the equations above for an equilibrium temperature  $T$ . Values used are as follows:  $\alpha/\epsilon = 0.12/0.2$  (Kapton tape layered aluminum with a 1 mil layer of Kapton tape);  $q_{solar} = 1368 \text{ W/m}^2$ ;  $q_{earth}$  (hot) =  $288 \text{ W/m}^2$ ;  $q_{earth}$  (cold) =  $177 \text{ W/m}^2$ ; albedo (hot) = 0.11; albedo (cold) = 0.63. We model our instrument frame as a box with 4 side panels, each with an area of  $0.15 \text{ m} \times 0.30 \text{ m} = 0.0045 \text{ m}^2$ , and a top and bottom each with area of  $0.15 \text{ m} \times 0.15 \text{ m} = 0.00225 \text{ m}^2$ . Our total instrument area is  $0.0225 \text{ m}^2$  and we assume  $\frac{1}{2}$  of the instrument is exposed to sunlight (during

the day, hot case only) and  $\frac{1}{2}$  of the instrument is exposed to earth irradiation (all the time).

With the parameters described above, we calculate expected interior operational temperatures of between  $-1^{\circ}\text{C}$  (cold case) and  $74^{\circ}\text{C}$  (hot case). These temperatures are within the stated operational temperature ranges for our electronic components.

### 1.3.2 - Thermal Testing Plan

To ensure thermal safety of the instrument, we will operate the instrument across this range of temperatures to ensure proper operation. We will enclose the entire instrument in a freezer to achieve the cold case temperature and we will heat the instrument with heating straps to achieve the hot case temperature.

If it is determined through testing that the instrument does not perform as required over the range of temperatures that will be encountered on flight, an active thermal control system may be used. Such a thermal control system would consist of a power resistor and thermistor readout and controlled through the microprocessor which is also responsible for data collection. If it is determined that active power control is required, we will ensure that the additional power supplied remains below the 15 W total power budget for a 'small' experiment with sufficient margin for safety.

## 2. Team Structure and Management

### 2.1 Team Organization and Roles

The team organization is outlined in the organization chart shown in figure 12 and the accompanying contact information table (table 1). The UVI-GREAT mission is designed from the ground up as both 1 - a student training and infrastructure development project and 2 - an instrumental development project. Since this project is the first of its kind at UVI and since the vast majority of the preparation for mission integration and testing has occurred during the travel restrictions of the COVID19 pandemic, the team is constructed of a combination of UVI students and former students, UVI faculty advisors, and collaborating contract engineers. A primary focus of this project is to transfer skills and develop lab instrumentation and procedures to make future experiments and testing easier to do and more efficient.

The UVI-GREAT team is led by UVI student (now graduated) Peter Jean-Baptiste. Mr. Jean-Baptiste is responsible for all aspects of equipment and component specification setting and procurement. Mr. Jean-Baptiste is also responsible for lab inventory, coordination and tasking oversight of other students in the lab. Student Kaheem Walters (Physics-21) is responsible for detector capability definition, detector design, and detector testing and

calibration. Ruel Mitchell (Applied-Math '20) is responsible for mechanical design and drawing as well as thermal analysis and thermal test design. Kervin Mathurin (Physics-21) is responsible for ground software design and testing. Joel Mwambungu (Physics-22) is responsible for flight software development and integration. Jordina Pierre (Physics-22) is responsible for GEANT gamma-ray instrument simulation and modeling. Derrick Thomas (Physics-22) is the lead fabrication technician. Stephanie Bullock (Physics-23) will lead communications development. The team is managed by engineer Trevor Palmer and is assisted by contract engineering support from Daniel Mera, An Nguyen, and Hien-Vo Bich. Collaborators Georgia Denolfo, George Suarez and Grant Mitchell from NASA/GSFC provide science and testing support. The team is advised by faculty advisor Professor David Morris and Professor Morris is assisted by UVI physics grants manager Ms. Orpha Penn in all administrative duties of the project including purchasing and hirings.

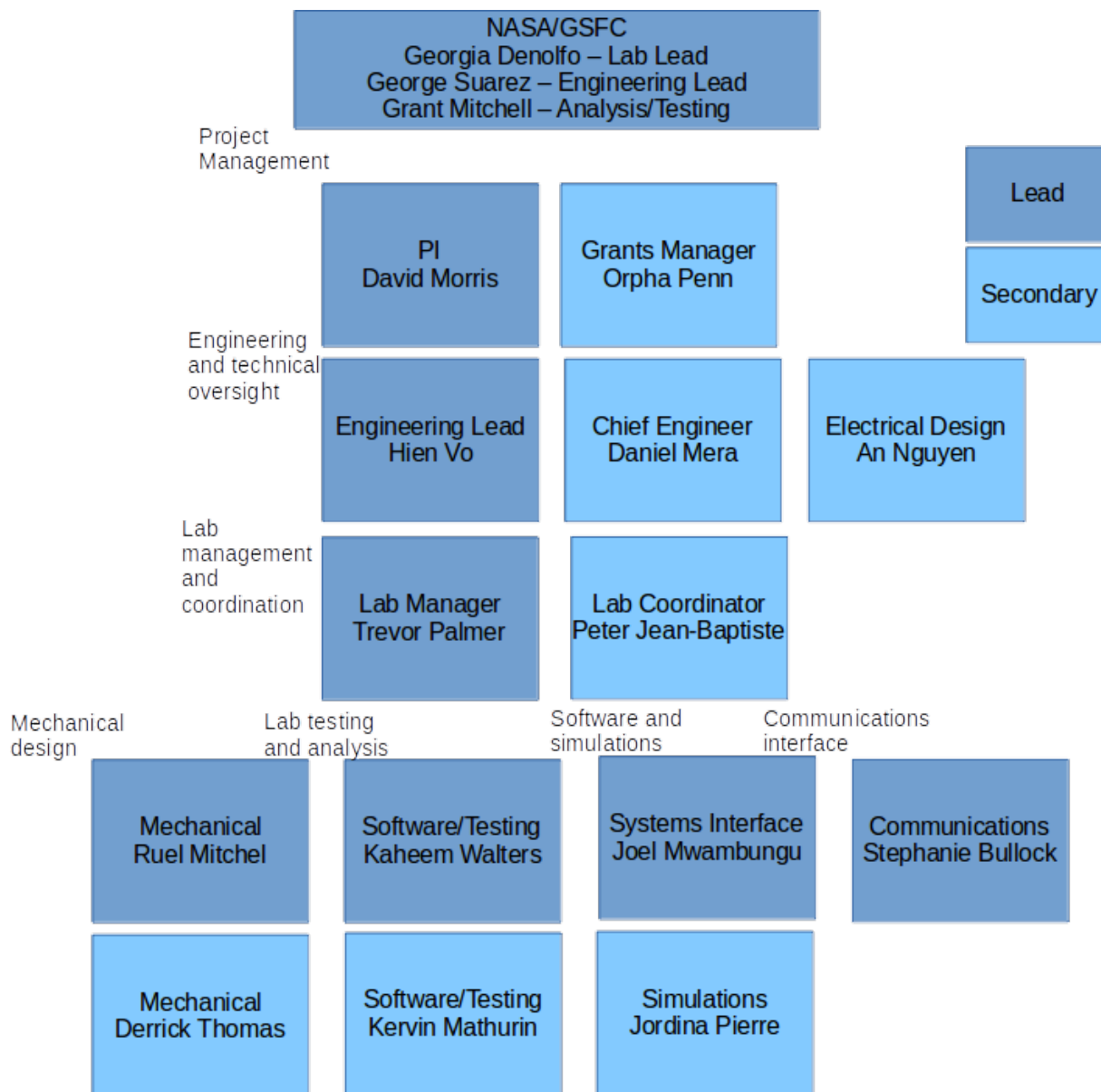


Figure 12 – Team Organizational Structure

Project Manager	Peter Jean-Baptiste Graduate	U of the Virgin Islands 2 John Brewers St. Thomas, USVI 00802	Pjeanbaptiste333@gmail.com
Mechanical Engineering Lead	Ruel Mitchell Graduate	U of the Virgin Islands 2 John Brewers St. Thomas, USVI 00802	ruelmitchell@gmail.com
Chief Engineer	Daniel Mera	U of the Virgin Islands 2 John Brewers St. Thomas, USVI 00802	wwwmera@gmail.com
Software/ Testing	Kaheem Walters Graduate	U of the Virgin Islands 2 John Brewers St. Thomas, USVI 00802	kaheemwalters@gmail.com
Mechanical Design	Derrick Thomas Jr. Undergraduate Student	U of the Virgin Islands 2 John Brewers St. Thomas, USVI 00802	Derrickthomasjr99@gmail.com
Electrical Design	An Nguyen	U of the Virgin Islands 2 John Brewers St. Thomas, USVI 00802	Nguyenngocan.spk@gmail.com
Software/ Testing	Kervin Mathurin Graduate Student	U of the Virgin Islands 2 John Brewers St. Thomas, USVI 00802	kervinmathurin@gmail.com
Engineering Lead	Hien Vo Bich	U of the Virgin Islands 2 John Brewers St. Thomas, USVI 00802	Hien.vb@vgu.edu.vn
Faculty Advisor	David Morris	U of the Virgin Islands 2 John Brewers St. Thomas, USVI 00802	Dmorris@uvi.edu
System Engineer	Trevor Palmer	U of the Virgin Islands 2 John Brewers St. Thomas, USVI 00802	Tpalmer8099@gmail.com
Systems Interface/ Communication	Joel Mwambungu Undergraduate Student	U of the Virgin Islands 2 John Brewers St. Thomas, USVI 00802	Joel.mwambungu@students.uvi.edu
Software Simulation/ Testing	Jordina Pierre Undergraduate Student	U of the Virgin Islands 2 John Brewers St. Thomas, USVI 00802	jordinapierre@gmail.com
Communication	Stephanie Bullock Undergraduate Student	U of the Virgin Islands 2 John Brewers St. Thomas, USVI 00802	Stephanie.Bullock@students.uvi.edu

Table 1 – Team contact information

## 2.2 Timeline and Milestones

It is anticipated that the integration and testing, flight and analysis activities will proceed as shown in the table below:

January 2022	Final hardware procurement, thermal testing of final instrument bus
February-March 2022	Flat-sat testing of instrument components
April-May 2022	Integration and Assembly
June 2022	Final Payload testing
July 2022	Final CDR document and stand-up review
August 2022	Buffer
September 2022	Launch
Oct-November 2022	Analyze data and prepare final report
December	Submit final report

Table 2 – Timeline and Milestones

## 2.3 Anticipated Participation in Integration and Launch operations

We anticipate that current UVI students on the team as well as newly recruited students will support integration and testing including thermal vacuum testing (as pandemic and public health conditions allow) during summer 2022. If allowed, UVI will plan to send a core team to participate in final integration and launch activities.

## 3. Payload Interface Specifications

### 3.1 Weight Budget and Power Budget

The following chart identifies the major components as well as the mass for each stated component based on blueprints/manuals provided by the manufacturers and uncertainty from secondary weighing. The payload currently has an estimated total mass inventory of 1643.99 +/- 157 grams and an expected power consumption budget of 6.78 +/- 0.79 watts. Both values are within the limits for a small HASP payload.

Component	Mass (g)	Estimated Mass (g) Error	Power (Watts)	Power Uncertainty
Microcontroller + Evaluation Board	190.18	10 (+/-)	3.5	0.05
SiPM Power Supply	5	1 (+/-)	0.00262	0.01
Board Power Supply	23	10(+/-)	1.5	0.05
Battery Pack	268	20 (+/-)	0.16	0.1
USB Hub	50	5 (+/-)	1	0.5
SiPM Board	112	10 (+/-)	0.27	0.03
RS 232 Board	18	1 (+/-)	0.35	0.05
Scintillator Crystal	370	50(+/-) **		**
Chassis (Mounts, Frame, etc.)	607.81	50 (+/-) **		**
<b>Total</b>	<b>1643.99</b>	<b>157(+/-)</b>	<b>6.78262</b>	<b>0.79</b>

Table 3 – Mass and power budget

### 3.2 Downlink Serial Data

We will utilize the RS232 serial link to monitor the status of the payload. The payload will use a TTL level shifter to interface the RS232 protocol's 12-volt logic with the 3.3-volt logic of our on-board microprocessor. The microprocessor will handle downlink serial communications constrained to the 1200 baud rate and default communication parameters defined by the HASP (8 data bits, no parity, 1 stop bit, no flow control). The downlink data will be sent at a rate of 264 bps per the 22 byte frame defined below, which falls within the data transfer limits (1200 baud) of the RS232 link.

Byte	Title	Description
1-2	Header	Beginning of the data record
3-10	Timestamp	Simple computer timestamp
11-18	Temperature	Temperature of internal components

19-20	Status	Indicates normal or fault event
21-22	Fault Type	Specifies the fault event
23-24	Footer	End of the data record

Table 4 – Data packet formatting

### 3.3 Uplink Serial Commanding

We will **not** be utilizing the RS232 interface for uplink serial commanding.

### 3.4 Analog Downlink

We will **not** be utilizing the analog downlink channels provided by the EDAC 516 interface.

### 3.5 Discrete Commanding

We plan to only utilize the two discrete commands (Power On/Off) provided by pins F & N of the discrete command line interface. If the serial downlink data indicates a fault listed in the data matrix, then a power on/off command will be requested to reset the payload - no additional discrete commands are required.

### 3.6 Payload Location and Orientation Request

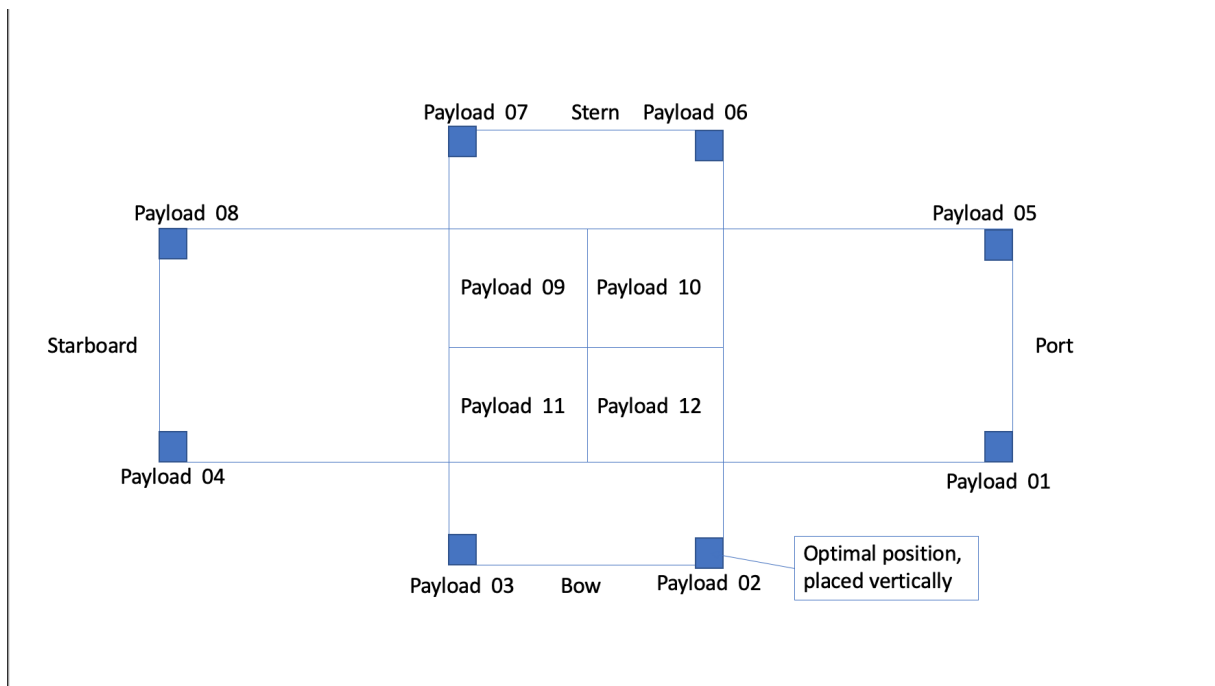


Figure 13 – payload location optimum location

Figure 13 displays the layout of the HASP. Payloads 1-8 are for small payloads such as our Instrument and 9-12 are for large payloads. Our instrument

requires an unobstructed view of the sky to avoid potential absorption or obstruction of x-rays and gamma-rays from the gondola frame. Each of the small payload options are the same length away from the center of the HASP and are on the same level. So, all small payload locations are suitable for our mission requirements. In addition, we require no additional serial discrete commanding channels besides the 2 on/off lines, so all small payload locations are suitable. Due to expected HASP camera mast positioning, payload slot 02 is requested as our optimal placement, but all small payload slots are acceptable.

### 3.7 Special Requests

The only hazardous materials list item that is included in our payload is a Li-Ion battery pack. The Li-Ion battery pack we plan to use is the AAC Clyde Optimus 30 Whr battery pack. This battery pack is space qualified for use aboard the International Space Station (ISS) and the certificate of conformance for compatibility with the ISS for manned space flight is included in the appendix. While the battery has not been explicitly UL certified to our knowledge, we refer to the attached certificate of conformance for manned space flight use to verify its safe use.

HASP 2022 Battery Hazard Documentation	
Batter Manufacturer	AAC Clyde Space
Batter Type	CS08109-01-02685 30Wh Battery 3 <sup>rd</sup> generation
Chemical Makeup	Li Ion
Battery modifications	No

Table 5 – Hazardous Materials Required Documentation

## 4. Preliminary Drawings and Diagrams

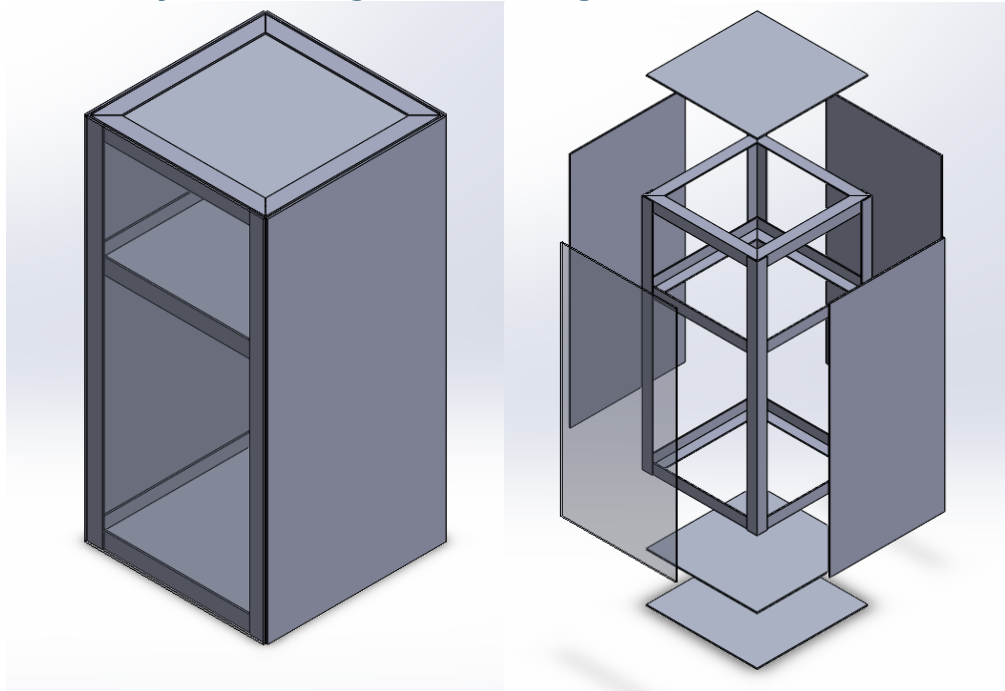


Figure 14 – 3-D rendering of 3-U UVI-GREAT configuration and exploded view

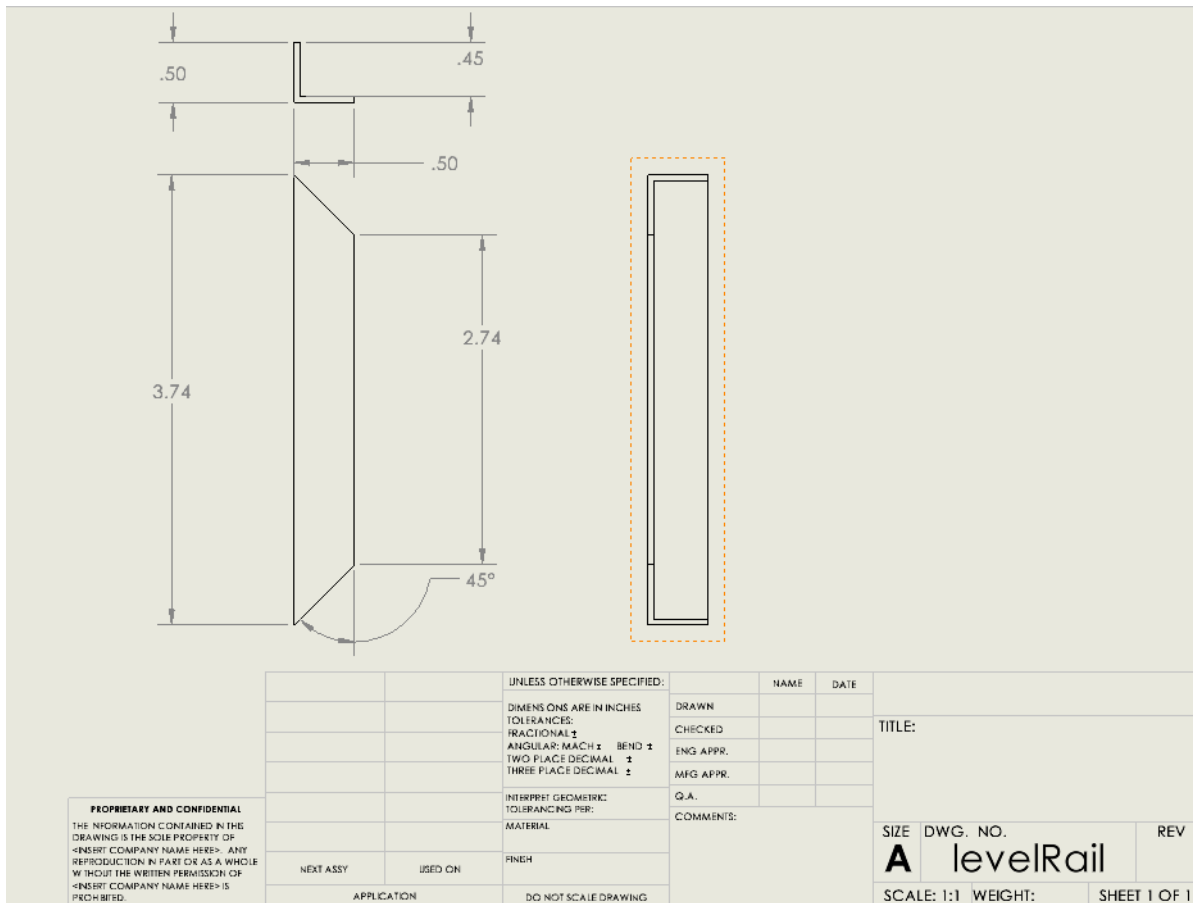


Figure 15 – Mechanical drawing of UVI-GREAT level rail used to secure base levels

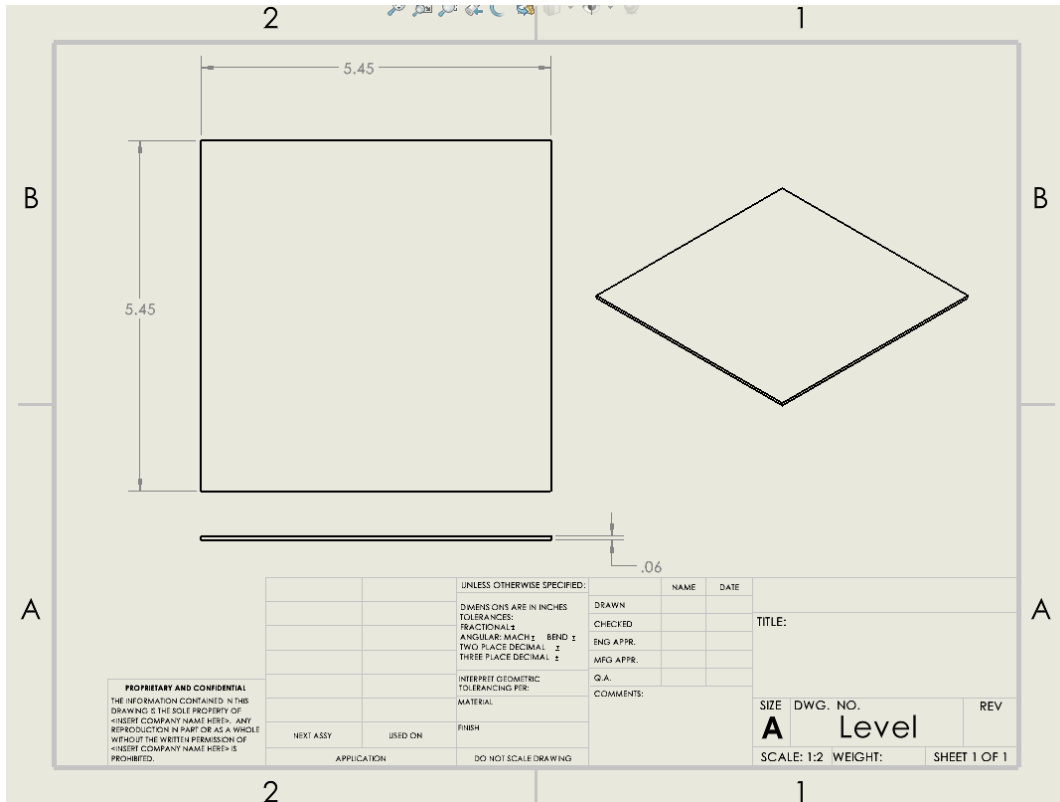


Figure 16 – Mechanical drawing of UVI-GREAT structure level

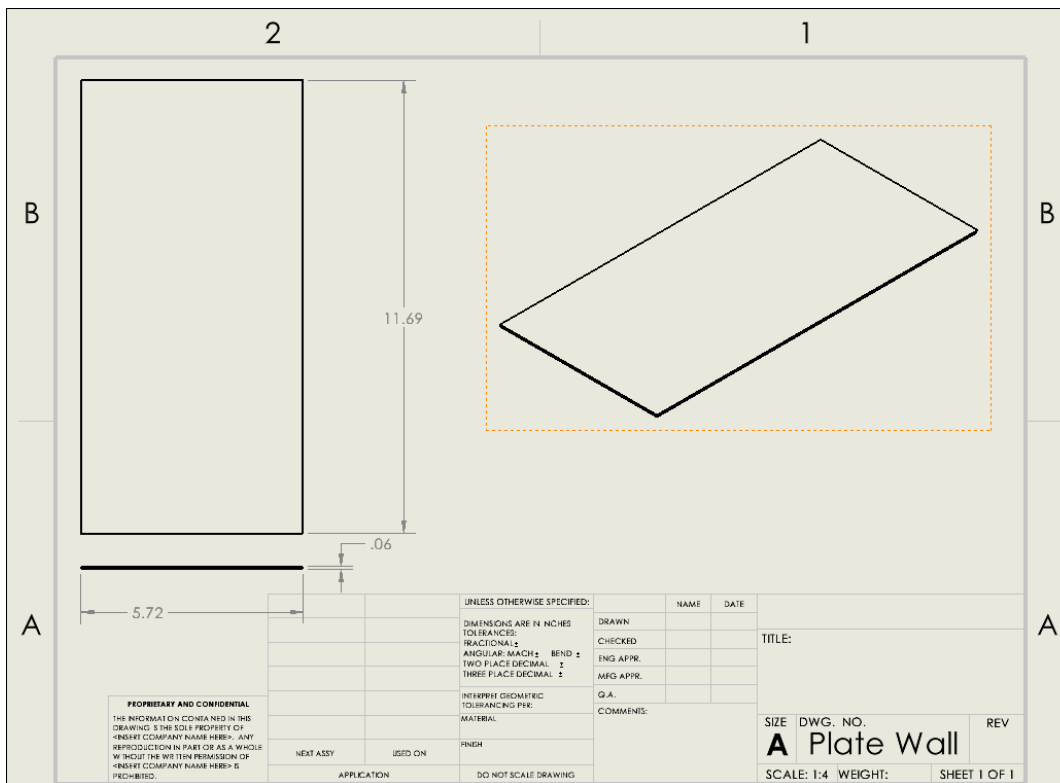


Figure 17 – Mechanical drawing of UVI-GREAT structure enclosing wall



# Appendix



## CS08109- 01-02685- Standalone 30Wh Battery 3rd Generation for Manned Flight ISS Compatibility Certificate of Conformance

COC-3866 Rev A

Date: 26 Nov 2021

**AAC Clyde Space Confidential**

AAC Clyde Space AB (publ) is registered in Sweden. Registration number 596677-0999. Registered office: Uppsala Science Park, Uppsala

Clyde Space Ltd, a subsidiary of AAC Clyde Space AB, is registered in Scotland. Registration number: SC285287. Registered office: Skypark 5, Glasgow

[www.aac-clyde.space](http://www.aac-clyde.space)

Copyright © 2021 Clyde Space Ltd. All rights reserved.

Clyde Space Ltd. is a subsidiary of AAC Clyde Space AB (publ) and operates under the trading name 'AAC Clyde Space'.

No part of the contents of this publication may be reproduced or transmitted in any form or by any means without the written permission of AAC Clyde Space.

AAC Clyde Space have taken care in the preparation of this publication but make no expressed or implied warranty of any kind and assume no responsibility for errors or omissions. No liability is assumed for incidental or consequential damages in connection with or arising out of the use of the information contained within this publication. The material in this document is for information only and is subject to change without notice.

AAC Clyde Space™ is a trademark of AAC Clyde Space. Other company, product or service names may be trademarks or service marks of others.

AAC Clyde Space AB (publ) is registered in Sweden. Registration number 556677-0599. Registered office: Uppsala Science Park, Uppsala

Clyde Space Ltd, a subsidiary of AAC Clyde Space AB, is registered in Scotland. Registration number: SC285287. Registered office: Skypark 5, Glasgow

[www.aac-clyde.space](http://www.aac-clyde.space)



Approval signatures

Rev	Author	Signed	Date	Approver	Signed	Date
A	S Wilson		26 Nov 2021	A Paditti		29 Nov 2021

Document control

Rev	Date	Section	Description of change	Reason for change
A	26 Nov 2021	All	First release	N/A



Contents

1 Statement of conformity .....	5
2 Test Results .....	6



CS08109 - 01 - 02685 - Standalone 30Wh Battery 3rd  
Generation for Manned Flight ISS Compatibility  
Certificate of Conformance

## 1 Statement of conformity

Serial number CS08109 conforms to the expected performance of Clyde Space Ltd product number 01 - 02685 - Standalone 30Wh Battery 3rd Generation for Manned Flight ISS Compatibility.



## 2 Test Results

Test	Result	Theoretical Equation
Capacity Test	Pass	N/A
Battery Current Telemetry Test	Pass	$0.008993 \times \text{ADC}$
Battery Voltage Telemetry Test	Pass	$14.662757 \times \text{ADC}$
3V3 Bus Voltage Telemetry Test	Pass	$0.004311 \times \text{ADC}$
3V3 Bus Current Telemetry Test	Pass	$1.327547 \times \text{ADC}$
5V Bus Voltage Telemetry Test	Pass	$0.005865 \times \text{ADC}$
5V Bus Current Telemetry Test	Pass	$1.327547 \times \text{ADC}$
Motherboard Temperature Telemetry Test	Pass	$(0.372434 \times \text{ADC}) - 273.15$
Daughterboard 1 Temperature Telemetry Test	Pass	$(0.397600 \times \text{ADC}) - 238.57$
Daughterboard 2 Temperature Telemetry Test	Pass	$(0.397600 \times \text{ADC}) - 238.57$
Daughterboard 3 Temperature Telemetry Test	Pass	$(0.397600 \times \text{ADC}) - 238.57$
Daughterboard 4 Temperature Telemetry Test	Pass	$(0.397600 \times \text{ADC}) - 238.57$
Thermal Cycling Performance	Pass	N/A
Post Thermal Reduced Test	Pass	N/A
Communications Node Operation	Pass	N/A
Inhibits Test	Pass	N/A
Over Voltage Test	Pass	N/A
Telemetry Commands	Pass	N/A
Heater Commands	Pass	N/A